Compartmentalized Development of the Chordae Tendineae and Anterior Leaflet of the Bovine Mitral Valve

Meghan Martin , Chih-Ying Chen , Timothy McCowan , Sarah Wells *

Posted Date: 5 March 2024

doi: 10.20944/preprints202403.0277.v1

Keywords: heart valves; extracellular matrix; remodeling; elastin; cardiac development; collagen; valvulogenesis

Article

Compartmentalized Development of the Chordae Tendineae and Anterior Leaflet of the Bovine Mitral Valve

Meghan Martin [1], Chih-Ying Chen [2,3], Timothy McCowan [2,4] and Sarah Wells [1,2,*]

[1] School of Biomedical Engineering, Dalhousie University, Halifax, Nova Scotia, Canada; MeghanMartin@dal.ca (M.M)
[2] Medical Sciences Program, Faculties of Science and Medicine, Dalhousie University, Halifax, Nova Scotia, Canada;
[3] Department of Pharmacology and Toxicology, University of Toronto, Toronto, Ontario, Canada; janecy.chen@mail.utoronto.ca (C.Y.C)
[3] Integrated Science Program, Faculty of Science, Dalhousie University, Nova Scotia, Canada; tm914510@dal.ca (T.M)
* Correspondence: sarah.wells@dal.ca

Abstract: There is increasing evidence that some adult mitral valve pathologies may have developmental origins involving errors in cell signaling and protein deposition during valvulogenesis. While early and late gestational stages are well-documented in zebrafish and small mammalian models, longitudinal studies in large mammals with a similar gestational period to humans are lacking. Further, the mechanism of chordae tendineae formation and multiplication remains unclear. This current study presents a comprehensive examination of mitral anterior leaflet and chordae tendineae development in a bovine model (with a gestational period of 9 months). Remarkably distinct from small mammals, bovine development displayed early branched chordae, with increasing attachments only until birth, while the anterior leaflet grew both during gestation and postnatally. Chordae also exhibited accelerated collagen deposition, maturation, and crimp development during gestation. These findings suggest that the bovine anterior leaflet and chordae tendineae possess unique compartmentalized processes of development despite being a continuous collagenous structure.

Keywords: heart valves; extracellular matrix; remodeling; elastin; cardiac development; collagen; valvulogenesis

1. Introduction

The increasing global prevalence of heart valve disease, propelled by an aging population and increased lifespan, is a growing health concern. Mitral valve pathologies, affecting approximately 24.2 million individuals worldwide and exhibiting an age-dependent increase in prevalence [1], not only compromises valvular function but also leads to left ventricular remodeling [2]. The current reliance on surgical interventions as the sole treatment for valve diseases further increases the strain on healthcare systems.

Several adult mitral valve pathologies have been linked to developmental defects during valvulogenesis [3–5]. For example, mutations in Dachsous cadherin-related 1 (DCHS1), the gene that codes for an atypical cadherin protein, have been identified in families with non-syndromic mitral valve prolapse [4,6,7]. Mutations in DCSH1 in developing mice are associated with loss of actin organization, one of the key steps in the mechanotransduction pathway [3]. Mice from these models show thickened fetal leaflets with abnormal extracellular matrix organization and eventually develop myxomatous mitral valve disease in adulthood [3,4]. These works show the clinical importance of understanding the processes and patterns of mitral valve formation throughout gestation.

 doi:10.20944/preprints202403.0277.v1

Fetal mitral valve development has been well-described in early and late gestational stages in many species, such as mice, rats, pigs, chicks, and zebrafish. In early gestation in humans [8], mice [9–11], chicks [12,13], and zebrafish [14–16], the formation of the endocardial cushions, comprised of a gelatinous extracellular matrix (ECM) surrounded by endocardial cells, sets the foundation for valve development. Endocardial cells undergo endothelial-to-mesenchymal cell transition (EMT) and migrate into the cushions, where they proliferate and differentiate into valvular interstitial cells (VICs) [8,16]. The endocardial cushions protrude into the lumen and change blood flow from oscillatory to unidirectional pulsatile flow [17,18], increasing shear stress and activating mechanotransduction pathways [18]. The mechanotransduction pathways have been extensively documented in the literature [13,19], particularly in zebrafish models [14,20–22].

Ongoing increases in flow and tension during gestation direct further development and maturation of the mitral apparatus. By late gestation in humans [23], mice [24–27], chicks [17,19,27–30], and pigs [31–33], the endocardial cushions are remodeled into the more mature fibrous leaflet and associated chordae tendineae through cellular proliferation, condensation, and deposition of fibrous ECM proteins [3,24–26,34,35]. Increasing tension becomes the dominating force on the primordial valve, activating pathways of thinning and ECM remodelling [18]. Collagen fibers accumulate and become organized within the atrialis, fibrosa/ventricularis, and part of the spongiosa layer [24,25,30,31]. Fully formed elastic fibers are not found in the leaflets until the second trimester (within the atrialis) and then continue to increase over gestation in pigs [31] and humans [36,37]. Notably, in mice, the anterior mitral valve leaflet forms while attached to the underlying myocardium, delaminating around embryonic day 15 [26]. The delaminated leaflet maintains a papillary muscle connection through a single chordae “bridge” [24,27] that does not divide into multiple, branched chordae tendineae until late gestation [5,24]. Interestingly, rats do not develop multiple branched chordae until after birth [39].

Postnatally the closure of fetal heart shunts elevates transvalvular pressures in the left side of the heart, resulting in significant changes to the anterior mitral valve leaflet structure, as observed in mice [3,24], pigs [31,33], and cattle [40]. These changes include increased thickness, collagen content, collagen crosslinking, and collagen alignment, accompanied by heightened cell remodeling activity, as indicated by elevated levels of alpha-smooth muscle actin, lysyl oxidase, and matrix metalloproteinases MMP2 and MMP9 [31–33,40–42]. This leads to the characteristic trilaminar organization of the leaflet after birth [31,33] in the same porcine models.

What is missing is our understanding of the mechanism and processes underlying mitral valve development in mid-gestation. While cellular activity is well characterized over this interval [3,5,17,19], ECM deposition and organization remain poorly characterized. Also missing is our understanding of valvulogenesis in large animal models with longer gestational periods, providing an extended timeframe for valve development. While late gestation in the porcine model is well-characterized [31–33], a comprehensive understanding of histological changes and ECM protein quantification over time in these larger mammals remains lacking. Moreover, the development of branched chordae tendineae in large animal models has received limited attention in the literature, aside from brief mention in studies on pigs [31] and humans [23,43] that reported the presence of some branched chordae tendineae in late gestation.

The objectives of this study were to characterize anatomical and histological changes in the mitral valve anterior leaflet and chordae tendineae in a large animal model (bovine). Like humans, cattle have a similar four-chambered heart structure, nine-month gestational period, substantial size, and similar transvalvular pressures [39], thus serving as an excellent model for characterizing mitral valvulogenesis across gestation. Bovine tissues are also commonly used in studies on cardiovascular mechanics and in tissue engineering where chemically-modified bovine pericardial tissues are used in the development of bioprostheses. Remarkably distinct from small mammals, branched chordae tendineae were present within first trimester where attachments increased only until birth while the anterior leaflet grew both during gestation and postnatally. Bovine chordae further demonstrated accelerated collagen deposition, maturation, and crimp development during gestation. However, elastic fibers appeared in the leaflet ahead of the chordae suggesting that elastic fiber deposition and

 doi:10.20944/preprints202403.0277.v1

organization is the final step of chordae formation. These findings suggest that the bovine anterior leaflet and chordae tendineae possess unique compartmentalized processes of development with distinct timelines of development despite them being a continuous collagenous structure.

2. Materials and Methods

2.1. Tissue Harvest and Anatomical Dimensions

Protocols for the harvesting of bovine (Bos taurus) tissues were approved by the University Committee on Laboratory Animals at Dalhousie University. Hearts from both male and female fetal calves were obtained from two local abattoirs immediately following slaughter. Gestational age was determined from the fetal crown-to-rump length (CRL) using the following equation [45]:

$$Gestational\ age\ =\ 8.4 + 0.087(CRL) + 5.46(CRL)^{\frac{1}{2}}$$

Fetuses ranged in age from 60 to 270 days gestation (full term). The mitral valve anterior leaflet and associated chordae were excised, laid flat, and photographed with a reference scale bar. Images were imported into image analysis software (ImageJ, National Institutes of Health, Bethesda, Maryland, USA). The freehand selection tool was used to outline the leaflet's perimeter to calculate the total leaflet area. The multipoint tool was used to determine the number of chordal attachments to the anterior leaflet.

2.2. Collagen Biochemical Analysis

For biochemical assays, whole anterior mitral valves were placed in phosphate-buffered saline (PBS) soaked gauze before being immediately stored in the -86°C freezer until testing. Upon thawing, a radial segment of the anterior leaflet (taken from free edge to fixed edge between the strut chordae attachments) and a segment of the strut chordae (from leaflet attachment to papillary muscle, no branches included) were excised and wet weights of the samples were recorded in mg. Wet weights of the samples varied based on gestational age but for the chordae ranged from approximately 1-15mg and for the leaflet 5-40mg. First trimester valves were too small to yield samples for biochemical assay, so this analysis includes only samples aged 106 days to 270 days (full term).

To measure the levels of acid and pepsin-soluble collagen, the Sircol™ Soluble Collagen assay (Biocolour, Carrickfergus, UK) were used according to the manufacturer's protocols. This form of collagen can be interpreted as newly synthesized collagen not sufficiently crosslinked into the network to resist solubilization. To isolate out the soluble collagen, tissue samples were placed in 0.1 mg/ml pepsin (Sigma-Aldrich, Oakville, ON) in 0.5M acetic acid overnight at 4°C and the supernatant used for the Sircol™ Soluble Collagen assay. The remaining tissue residues underwent the Sircol™ Insoluble Collagen assay (Biocolour, Carrickfergus, UK) following the manufacturer's protocol. Insoluble collagen is interpreted as mature crosslinked collagen. The residues were denatured at 65°C for three hours in acetic acid causing all tissue to breakdown and to crosslinked collagen to release into solution.

All samples were assayed in duplicate and compared to a set of blanks (water) and known concentration of standards comprised of bovine collagen. Following each assay, a microplate reader (Varioskan LUX; Thermo Scientific, Waltham, MA) was used to measure the dye absorbance of each prepared plate at a wavelength of 555nm. Collagen content was calculated from the sample absorbance and normalized against wet tissue weight to get collagen concentration in μg/mg wet tissue weight.

2.3. Histology

One-half of the anterior leaflet with associated chordae tendineae was cut from fetal samples in the second and third trimesters (91-270 days gestation). For first trimester samples (0-90 days gestation) the whole anterior leaflet and chordae were used due to their small size. Samples were fixed (10% buffered neutral formalin), embedded in paraffin, and sectioned into 4μm serial transverse longitudinal sections. To examine collagen alignment and crimp, sections were stained with

 doi:10.20944/preprints202403.0277.v1

picrosirius red and hematoxylin. To visualize cells and the localization of ECM proteins, sections were stained with Russell-Movat Pentachrome Stain Kit (Statlab, Texas, USA) using the manufacturer's instructions. This kit stains collagen yellow-orange, mature elastin dark purple, muscle tissue and blood cells red, glycosaminoglycans in blue-green and cell nuclei in dark red-purple. Movat-stained slides were imaged using a Pannoramic MIDI II and viewed with the Caseviewer software (3DHistech, Budapest, Hungary).

2.4. Collagen Crimp Analysis

Images of picrosirius red stained section were taken using a Nikon Eclipse E600 light microscope equipped with a polarizer and an AmScope 10MU1400 digital camera. Images were taken at the X40 objective along the circumferential direction of the leaflet and radial length of the chordae. Collagen crimp was characterized (as described previously [46–48] with minor modifications) by (a) crimp wavelength (peak to peak distance of one crimp period) and (b) the percentage of tissue area that was crimped. Briefly, crimp wavelength was analyzed in ImageJ where a 4-quadrant grid (0.01mm^2/square) was placed over the image, and two areas per grid were measured. A straight line in the middle of the fiber was drawn and all the crimp peaks parallel to the line were measured over that distance. The crimp wavelength measurements were averaged across all grids to give one value per image. Crimp area was measured by placing a 600μm^2/square grid overtop the same images and grid points were counted as (i) in contact with crimped tissue, (ii) uncrimped tissue, and (iii) empty space (which was then omitted from total grid count). The ratio of crimped grid points to the total grid count was used to calculate the percentage of crimped chordal area.

2.5. Statistical Analysis

To assess the changes in each parameter during fetal development, data were plotted as a function of gestational age in days and fitted with a linear least-squares regression. Each data point represents n = 1 animal. The regression was considered significant when $p < 0.05$. To compare the rate of change within any single parameter during fetal development between tissues (chordae versus leaflet), the regression slopes were compared using an analysis of covariance (ANCOVA). Differences between the slopes were considered significant when $p < 0.05$. For the soluble collagen data there was no significant change with gestational age in chordae or leaflet so comparisons between those tissues were made using the gestational averages using an unpaired two sample t-test. All statistical analyses were conducted using R [49]: specifically, the car package [50], mvnormtest package [51], the DescTools package [52], and the devtools package [53].

3. Results

3.1. Chordae Division Occurs Only During Gestation Whereas Leaflet Area Continues to Increase Postnatally

The anterior mitral valve leaflet underwent significant increases in area and number of chordae tendineae attachments during gestation (Figure 1). Anterior leaflet area increased over gestation from 64 days (4.33e^{-7} mm^2) to 270 days (2.98 mm^2) yet remained 3 magnitudes of order lower than the adult average (1054 + 185 mm2) (Figure 1F). The adult averages given here are from our previously published data using heifers (never-pregnant, sexually mature female cattle) [54,55]. Chordae attachments also increased linearly over during gestation from 60 days (4 attachments) to 270 days (83 attachments) (Figure 1E). However, unlike leaflet area, the number of chordae attachments reaches adult-like numbers (72 + 13) by full term.

Preprints.org (www.preprints.org) | NOT PEER-REVIEWED | Posted: 5 March 2024 doi:10.20944/preprints202403.0277.v1

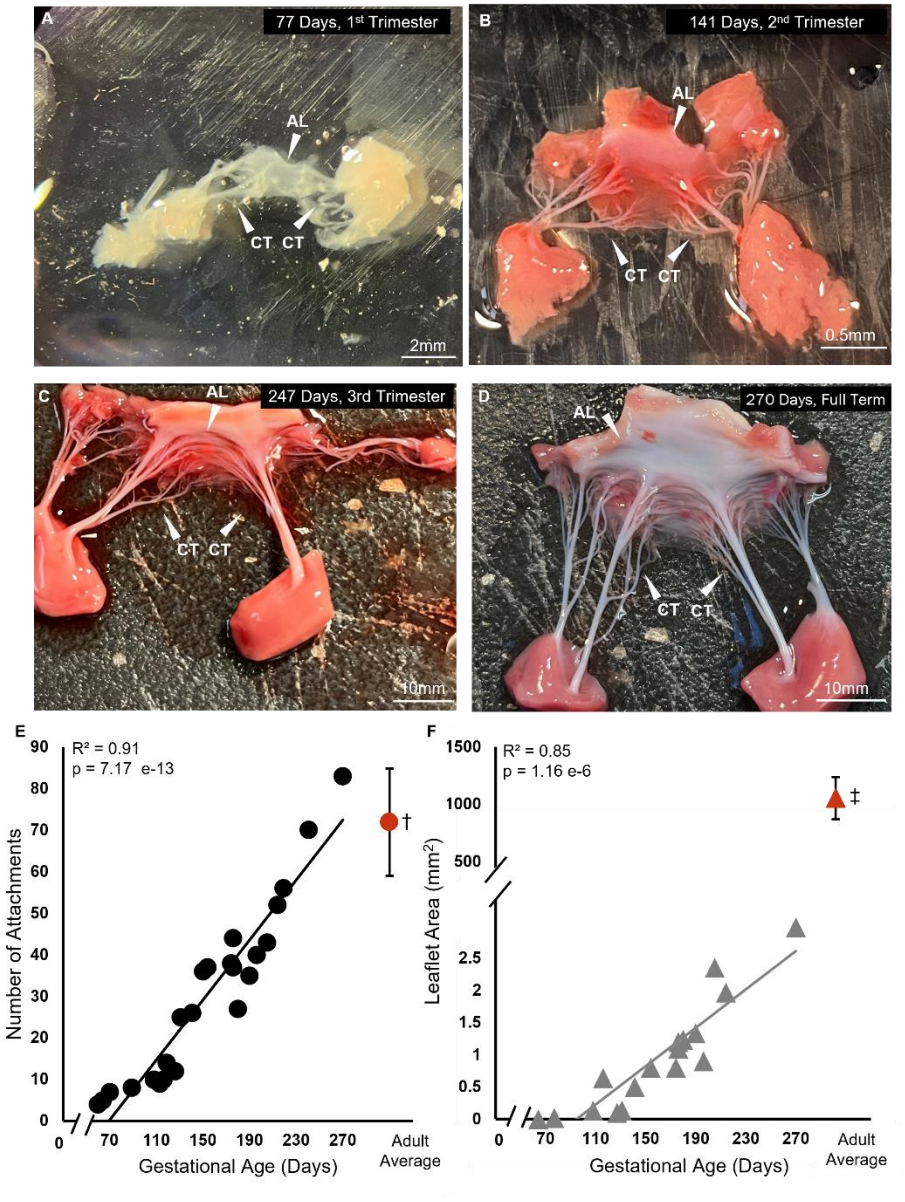

Figure 1. Branched chordae are present within first trimester of bovine mitral valve development with chordae number and leaflet area increasing throughout gestation. **A-D**: Representative images of bovine fetal mitral valve anterior leaflets and chordae tendineae from first trimester (77 days gestation), second trimester (141 days gestation), third trimester (247 days gestation), and full-term (270 days). White arrows denote the anterior leaflet (AL) and chordae tendineae (CT). **E:** Number of chordae tendineae attachments plotted as a function of gestational age (black circles) showing a significant correlation between these variables. Each data point represents n = 1 animal. †The average value (±SD, n=13) from adult animals taken from Scott 2016 [54] is shown in red for comparison to fetal data. **F:** Anterior leaflet area in mm^2 plotted as a function of gestational age in days (gray triangles) showing a significant correlation between these variables. ‡The average value (±SD, n=11) from adult animals, taken from Wells et al, 2012 [55] is shown in red for comparison to fetal data. Note the axis breaks on both graphs.

3.2. In Leaflet and Chordae, Mature Collagen Content Increases Over Gestation Despite Unchanged Levels of Newly Synthesized Collagen

Biochemical analysis of both soluble and insoluble collagen showed unexpected patterns (i) during gestation and (ii) between the leaflet and chordae. Soluble "newly synthesized" collagen concentration was surprisingly unchanged over gestation in both tissues, with consistently higher

 doi:10.20944/preprints202403.0277.v1

levels in the chordae (averages over gestation in chordae = 5.76 + 0.89 μg/mg vs leaflet = 2.03 + 1.34 μg/mg, p = 1.51e^{-8}, Figure 2A). By contrast, the concentration of insoluble "mature" collagen increased linearly over gestation in both the leaflet and chordae, but at a faster rate in the chordae (Figure 2B).

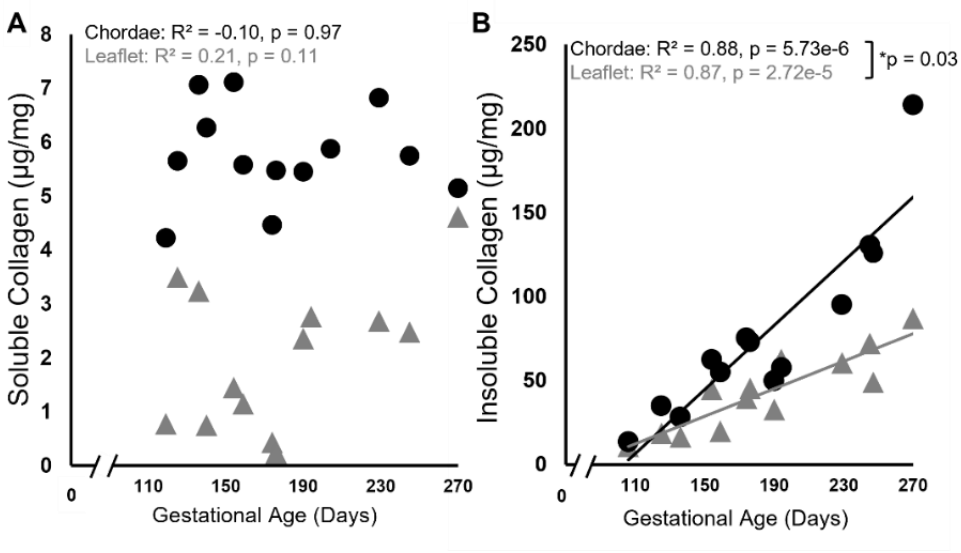

Figure 2. Levels of soluble (newly synthesized) collagen remain unchanged during gestation while insoluble (mature) collagen content increases in both the anterior leaflet and chordae tendineae. Concentration of soluble (**A**) and insoluble (**B**) collagen (in μg/mg wet weight) of the anterior leaflet (gray triangles) and strut chordae tendineae (black circles) as a function of gestational age. Each data point represents n = 1 animal. Note the break in the x-axis both graphs. Significant regression lines are shown as solid lines and ($p<0.05$). *Denotes significant difference in slope ($p=0.03$) values analyzed via analysis of covariance.

3.3. Collagen Crimp Develops Earlier in the Chordae Versus the Leaflet

There were also changes to collagen crimp in leaflet and chordae during gestation, with the chordae leading the leaflet in crimp development. Figure 3 shows representative bright field and polarized light images of the picrosirius red stained leaflet and chordae from fetuses at 70 gestational days (Figure 3A), 111 days gestational (Figure 3B), 202 days gestational (Figure 3C), and 270 days gestational, full term (Figure 3D) where increasing crimp wavelength over gestation is visualized in both tissues. Measurements of crimp wavelength are shown in Figure 4B.

Preprints.org (www.preprints.org) | NOT PEER-REVIEWED | Posted: 5 March 2024 doi:10.20944/preprints202403.0277.v1

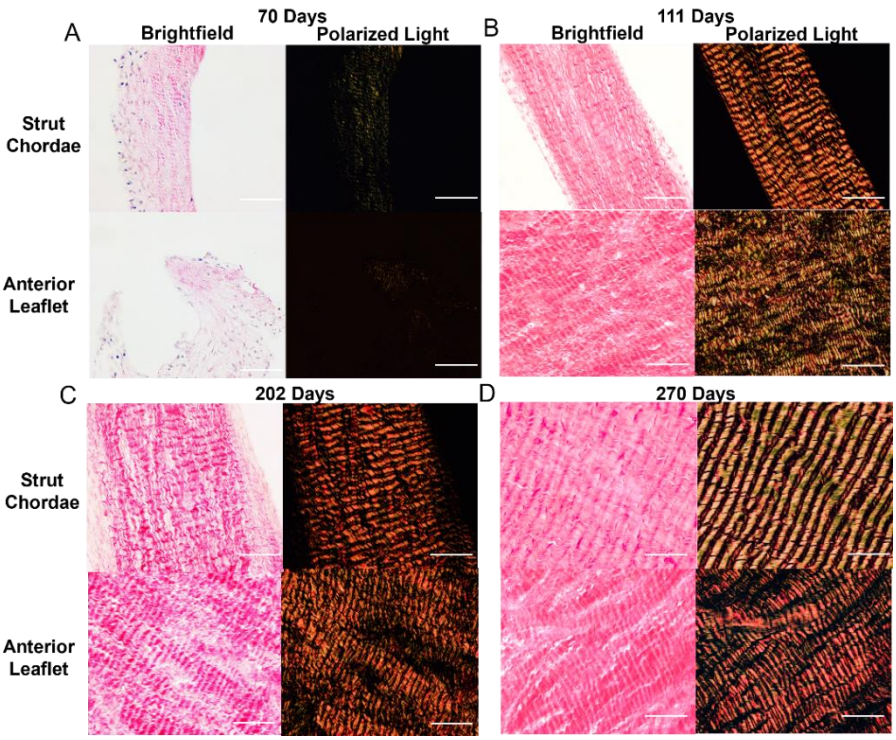

Figure 3. Collagen crimp wavelength increases throughout gestation in both the anterior leaflet and chordae tendineae. **A-D:** Bright field and polarized light images of the mitral anterior leaflet and strut chordae from first trimester (70 days gestation), second trimester (111 days gestation), third trimester (202 days gestation), and full-term valve (270 days gestation). Images taken at 400x. Scale bar, 0.05mm.

Leaflet and chordae showed identical linear increases in the percent of crimped collagen over gestation (Figure 4A). Collagen crimp wavelength also increased linearly during gestation in both the leaflet and chordae but with a slightly higher rate of increase in the chordae (Figure 4B).

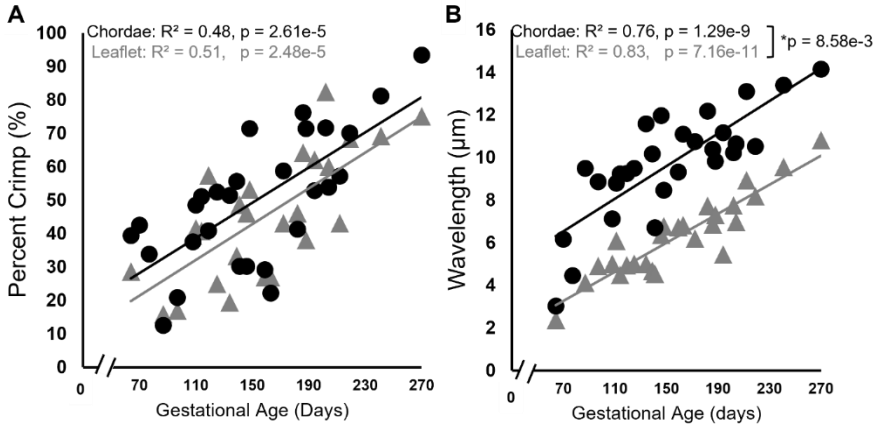

Figure 4. Collagen crimp is established throughout gestation in both the anterior leaflet and chordae tendineae. Percent area of crimped tissue (**A**) and collagen crimp wavelength in μm (**B**) of the anterior leaflet (gray triangles) and strut chordae tendineae (black circles) as a function of gestational age. Each data point represents n = 1 animal. Note the break in the x-axis for both graphs. Significant regression lines are shown as solid lines and ($p<0.05$).] *Denotes significant difference in slope ($p<0.05$) values analyzed via analysis of covariance.

 doi:10.20944/preprints202403.0277.v1

3.4. Bovine Mitral Chordae and Leaflet Collagen Fibers Are Laid Down in Their Adult-Like Orientations

Movat pentachrome staining surprisingly revealed no major changes to collagen fiber orientation in the leaflet and chordae throughout gestation (Figure 5). The leaflet was comprised of collagen aligned circumferentially (Figure 6A, 6C, and 6E) while the chordae were dominated by longitudinally-aligned collagen as observed in mature animals (Figure 6B, 6D and 6F). Sparse staining of glycosaminoglycans and many cell nuclei were present in leaflet and chordae throughout gestation (Figure 5 and 6).

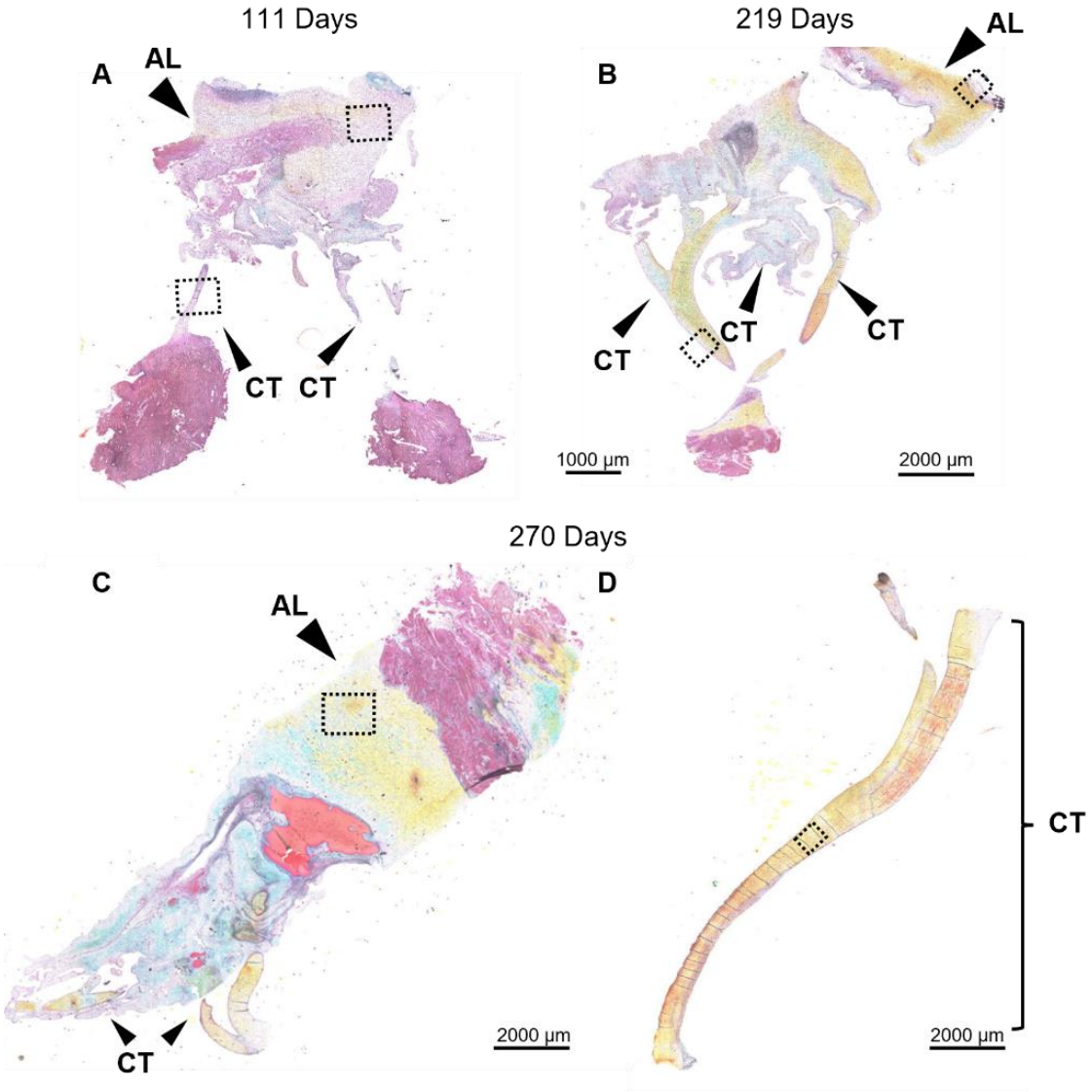

Figure 5. Throughout second trimester to full term the anterior leaflet and chordae tendineae are comprised predominantly of collagen. **A-D**: Representative images of extracellular matrix staining (Movat Pentachrome) from early second trimester (111 days gestation), third trimester (219 days gestation), and full term (270 days). Boxes show areas that are magnified in Figure 6. Black arrows denote the anterior leaflet (AL) and chordae tendineae (CT). Collagen is stained yellow-orange, elastic fibers dark purple, muscle tissue and blood cells red, glycosaminoglycans in blue-green and cell nuclei in dark red-purple. Scale bar varies per image.

 doi:10.20944/preprints202403.0277.v1

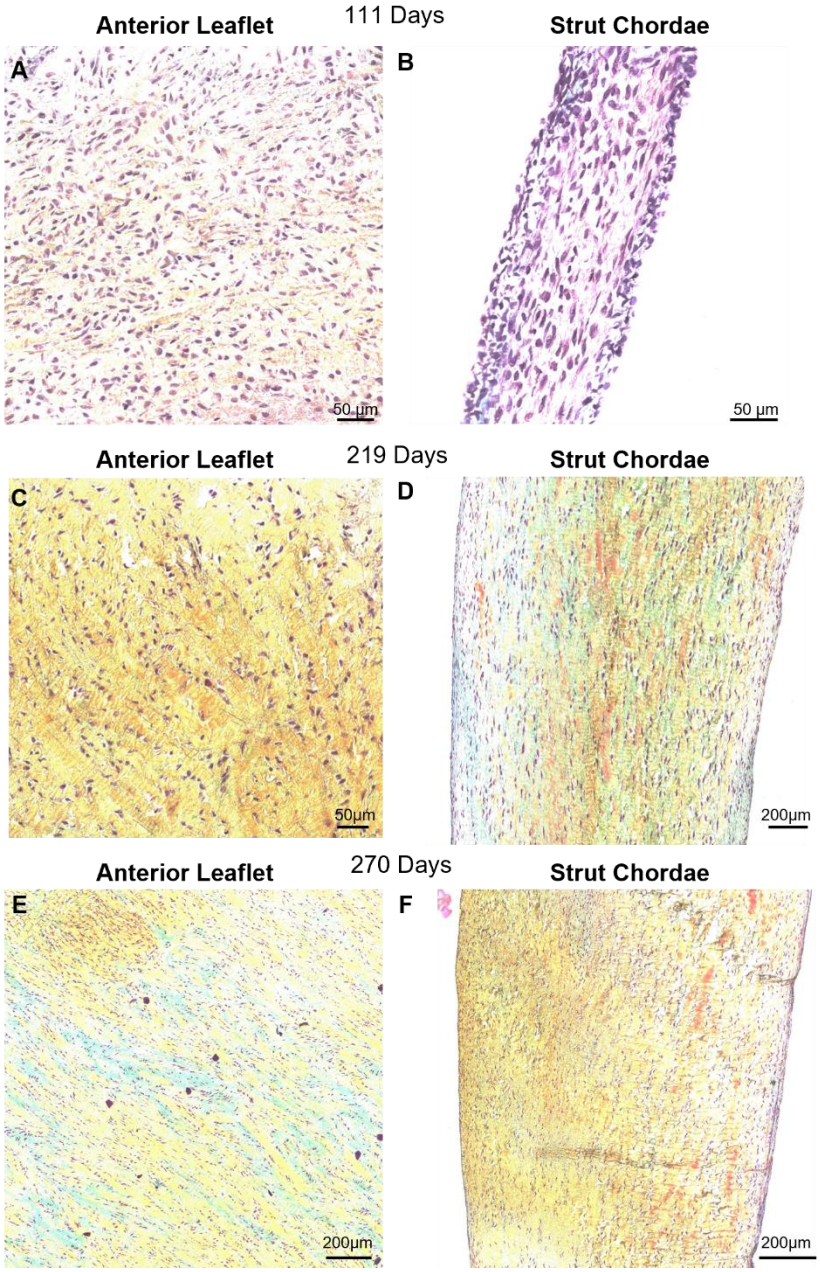

Figure 6. Throughout gestation there were no major changes to collagen fiber orientation in the anterior leaflet or chordae tendineae. Magnified sections images of Movat Pentachrome-stained mitral anterior leaflets (**A, C,** and **E**) and strut chordae tendineae (**B**, **D**, and **F**). **A** and **B**: early second trimester (111 days gestation). **C** and **D**: third trimester (219 days gestation). **E** and **F**: full term (270 days). Collagen is stained yellow-orange, elastic fibers dark purple, muscle tissue and blood cells red, glycosaminoglycans in blue-green and cell nuclei in dark red-purple. Scale bar varies per image.

3.5. Contrary to Collagen Patterns, Elastic Fibers Appear in the Leaflet Ahead of the Chordae

There were also differential patterns of elastic fiber deposition in the leaflet and chordae over gestation. Elastic fibers first appeared in the leaflet during the early 2nd trimester (111 days, Figure 7A) near the fixed edge. Elastic fibers accumulated through gestation, extending into the rest of the leaflet (Figure 7C, 7E, and 7G). By contrast, elastic fibers were not present in the chordae during 2nd trimester (Figure 7B), appearing only sparsely at the outer edges of the chordae in early 3rd trimester (212 days, Figure 7D) with fibers increasing in density and length until full term (Figure 7F and Figure 7H). By late gestation, elastic fibers were also present within the bulk of the chordae (Figure 7F and Figure 7H).

 doi:10.20944/preprints202403.0277.v1

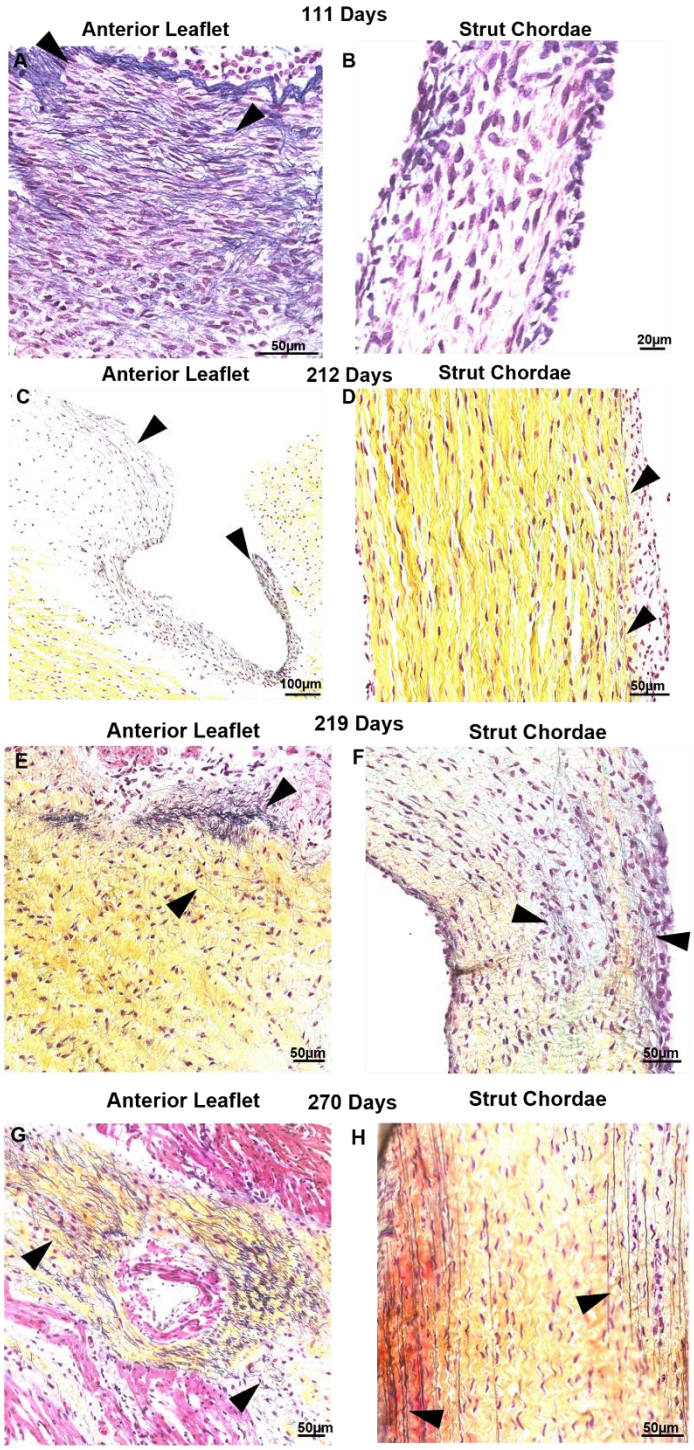

Figure 7. Elastic fibers appear first in the anterior leaflet before being deposited within the chordae tendineae. Representative images of elastic fibers in Movat Pentachrome-stained mitral anterior leaflet (**A, C, E**, and **G**) and chordae strut chordae tendineae (**B, D, F**, and **H**) throughout gestation. **A** and **B**: valve in early second trimester (111 days gestation). **C** and **D**: third trimester (212 days gestation). **E** and **F**: third trimester (219 days gestation). **G** and **H**: full term (270 days). Black arrows denote the presence of elastic fibers. Collagen is stained yellow-orange, elastic fibers dark purple, muscle tissue and blood cells red, glycosaminoglycans in blue-green and cell nuclei in dark red-purple. Scale bar varies per image.

 doi:10.20944/preprints202403.0277.v1

4. Discussion

This study has described, for the first time, the structural changes in the mitral valve anterior leaflet and chordae tendineae during fetal development in a large animal model with a gestation similar in length to that of humans. We found that — in striking contrast to small mammals — bovine mitral valve chordae tendineae rapidly develop over gestation, achieving their adult-like architecture by full term. This was accompanied by a rapid accumulation and maturation of ECM that outpaced that in the leaflet. Despite the continued expansion of leaflet area post-partum, the number of chordae attachments remains unchanged, suggesting the mechanism driving chordae division is active only during fetal development. Thus, despite a nearly continuous collagen fiber architecture between the mitral valve anterior leaflet and chordae tendineae, their development appears compartmentalized, each growing and maturing along independent timelines.

The main difference noted in fetal mitral valve formation between large and small mammals was in anatomical development. In mice, the anterior leaflet develops while remaining predominantly attached to the underlying myocardium [26,38]. Further, branched chordae tendineae are not formed until late gestation in mice [35] and postpartum in rats [39]. This has been attributed to the lower ventricular pressures during fetal development in small mammals, reducing the need for chordae during gestation [39]. While our bovine model demonstrated similar anterior leaflet attachment to the myocardium, this was only during the early first trimester and, contrary to in mice, branched chordae were present at this time. Branching and multiplication of chordae continued throughout gestation until the adult-like architecture (i.e., number of attachments to the anterior leaflet) was reached by full term. If the emergence of chordae is indeed linked to ventricular pressure, a threshold of ventricular pressure (and local tissue tension) may be required for chordae formation. If that is the case, this threshold is reached in large mammals during early development (first trimester) compared to small mammals (late gestation).

In the mitral valve of small mammals, collagen fibers are first laid down without a primary orientation before becoming more oriented within late gestation [25,30]. In our bovine model, collagen fibers were laid down in their adult orientation in the fetal anterior leaflet and chordae tendineae. At the fixed edge of the leaflet, collagen was predominantly oriented in the circumferential direction throughout gestation as it is in adults [56]. Similarly, in the chordae collagen alignment was predominantly longitudinal throughout gestation as it is in adults [57]. This further suggests that in large mammals, the requirement for a functional mitral valve occurs earlier in gestation.

Not surprisingly, the concentration of insoluble, mature collagen increased over gestation in both the leaflet and chordae. This change parallels increasing gene expression and presence of collagen seen in developing valves in other species as demonstrated through RT-qPCR, picrosirius red staining and immunohistochemistry [24,25,27,30,32,38,58–60]. Mature collagen accumulation in the chordae outpaced that in the leaflet, again reflecting the differential development of these tissues, with chordae tendineae undergoing rapid development during gestation.

The higher levels of soluble collagen in the chordae throughout gestation further reflect the differential development of the chordae versus the leaflet. Yet, while the levels were higher in the chordae there was no change in these concentrations over gestation in either tissue. Further, levels of soluble collagen were surprisingly low in both tissues. This is unexpected in developing fetal collagenous tissues which require collagen deposition for their formation. Procollagen molecules are synthesized within the rough endoplasmic reticulum before being released into the cytosol where they self-assemble into trimers, forming the collagen molecule. After excretion from the cell and post-translational modifications, soluble collagen molecules are deposited and crosslinked by the enzyme family of lysyl oxidases forming insoluble collagen fibrils. Many of these crosslinked fibrils bundle together to form the larger collagen fibers [61]. The accumulation of insoluble collagen in fetal chordae and leaflet, with unchanging concentrations of soluble collagen, suggests an elevated rate of collagen crosslinking during gestation, possibly via an upregulation of lysyl oxidase. The faster accumulation of mature collagen in the chordae may correspond to increased lysyl oxidase activity in comparison to that in the leaflet.

 doi:10.20944/preprints202403.0277.v1

Similar patterns during gestation were seen with collagen crimp wavelength, with its development occurring at a faster rate in the chordae versus the leaflet. While the exact mechanism of crimp formation remains unknown [62], it is suggested that cellular contraction triggered via mechanotransduction leads to the formation of crimp [63], with crimp wavelength increasing as tissues grow and elongate in the fiber direction [62,64,65]. While collagen crimp developed at the same rates throughout gestation in the bovine leaflet and chordae, we saw consistently longer wavelengths in the chordae. One explanation is that collagen crimp formation and lengthening begin earlier in the chordae (or at least earlier than the interval examined). This aligns with our previous observations above suggesting that the chordae are leading the leaflet in developmental maturation.

There are interesting parallels between the developing fetal mitral valve and the simultaneous remodeling of the maternal mitral valve during pregnancy. Both show an increase in leaflet area and the number of chordae attachments over gestation. In terms of collagen structure, both the maternal and fetal leaflets demonstrated an increase in crimp wavelength over gestation [46]. Similarities are also observed in collagen remodeling in both fetal and maternal valves: a rapid accumulation of insoluble, crosslinked collagen with extremely low concentrations of newly-synthesized soluble collagen [46]. This similarity suggests that an upregulation of lysyl oxidase activity may be an important mechanism in both maternal valve remodelling and fetal valve development. Further work on fetal and maternal valves should examine lysyl oxidase activity. High-performance liquid chromatography techniques also would provide direct analysis of the changing crosslinks types over gestation.

While the chordae led the leaflet in collagen deposition, maturation, and crimp formation, the leaflet led the chordae in terms of elastic fiber development. Elastic fibers first appeared near the fixed edge of the leaflet early in the second trimester, then accumulated into the rest of the leaflet over remaining gestation. By contrast, elastic fibers did not appear in the chordae until the third trimester. Thereafter, chordae elastic fibers rapidly accumulate at the outer layers reaching an adult-like appearance [54,57] by full term. The formation of this elastic fiber "jacket" may signal the end of chordae multiplication, as the number of chordae becomes fixed after birth. This is sensible as the elastin gene is turned off at maturity [66,67] and if chordae were to continue dividing into adult life, an elastin jacket could not be synthesized to arrest chordae division. Immunohistochemistry for the specific elastic fiber components (fibrillins, tropoelastins) in earlier gestation fetal calves would better elucidate the time course of elastic fiber assembly in the developing mitral valves.

The observed differential development of the bovine fetal mitral valve leaflet and chordae tendineae supports previous work in chick and mice models that have suggested a compartmentalized cell signalling in these tissues [27,68,69]. Distinct populations of cells in the developing endocardial cushions [68] direct a tendon-like development in the chordae versus a more cartilaginous-like development in the leaflet [27]. Specifically, leaflet-forming cells are responsive to bone morphogenetic protein 2 (BMP2) that induces expression of the cartilage markers sox9 and aggrecan, whereas chordae-forming cells are responsive to fibroblast growth factor 4 (FGF4) that induce the expression of tendon markers scleraxis and tenascin [68]. Interestingly, other FGF proteins have been shown to downregulate elastin expression [70,71]; raising the possibility that FGF expression in the chordae may be suppressing elastic fiber synthesis in early development. The appearance of elastic fibers during third trimester in the chordae may be triggered by increasing glucocorticoids [72], as they increase elastin gene expression [73,74] and may override the suppressive signal from FGF. Immunohybridization studies conducted in the bovine model are needed to determine if tendon-associated markers such as FGF are present in the developing bovine chordae.

5. Conclusions

In summary, this study demonstrated compartmentalized development of the mitral valve anterior leaflet and chordae tendineae in a bovine model – differing from that in small mammals with shorter gestational periods. Elucidating the mechanisms of mitral valve development over a longer gestation (like humans) could aid in identifying important congenital defects in valve development.

These findings could also inform the design criteria for developmental engineering of load-bearing tissues.

Author Contributions: Author contributions: M.L.M. and S.M.W. conception and design of research; M.L.M. and S.M.W. analyzed data; M.L.M. and S.M.W. interpreted results of experiments; M.L.M. prepared figures; M.L.M. and S.M.W. drafted manuscript; M.L.M. and S.M.W. edited and revised manuscript; M.L.M. and S.M.W approved final version of manuscript; M.L.M., C.Y.C, and T.M.M performed experiments.

Funding: Operational funds to S. M. Wells were provided by the Natural Sciences and Engineering Research Council of Canada (NSERC*), and the Faculty of Medicine, Dalhousie University. M. Martin was supported by the Heart and Stroke Foundation of Nova Scotia, and NSERC Postgraduate Scholarships (Canada Graduate Scholarship – Masters, and Vanier PhD Scholarship). *NSERC Discovery Grant, School of Biomedical Engineering, 229753-2013-RGPIN.

Institutional Review Board Statement: The animal study protocol was approved by the University Committee on Laboratory Animals (UCLA) of Dalhousie University (protocol code I23-35, 10/03/2023).

Data Availability Statement: All datasets will be made publicly available at the time of publication and are accessible at request of the corresponding author.

Acknowledgments: The authors would like to thank Darren Cole (School of Biomedical Engineering, Dalhousie University) and Curtmar Meats for supplying and retrieval of bovine tissues, Ashley Kervin (Department of Oral and Maxillofacial Sciences, Dalhousie University) for training and expertise in histological technique, Dr. Keith Brunt (Department of Pharmacology, Dalhousie University) for aid in imaging, Dr. Brendan Leung (Applied Oral Sciences, Dalhousie University) for use of the Varioskan LUX, and Dr J. Michael Lee (School of Biomedical Engineering, Dalhousie University) for valuable input on the study. The authors acknowledge that this work was conducted in Mi'kma'ki, the unceded territory of the Mikmaq people.

Conflicts of Interest: No conflicts of interest, financial or otherwise, are declared by the author(s).

References

1. Coffey, S.; Roberts-Thomson, R.; Brown, A.; Carapetis, J.; Chen, M.; Enriquez-Sarano, M.; Zühlke, L.; Prendergast, B.D. Global Epidemiology of Valvular Heart Disease. *Nat Rev Cardiol* **2021**, *18*, 853–864, doi:10.1038/s41569-021-00570-z.
2. Delling, F.N.; Noseworthy, P.A.; Adams, D.H.; Basso, C.; Borger, M.; Bouatia-Naji, N.; Elmariah, S.; Evans, F.; Gerstenfeld, E.; Hung, J.; et al. Research Opportunities in the Treatment of Mitral Valve Prolapse. *J Am Coll Cardiol* **2022**, *80*, 2331–2347, doi:10.1016/j.jacc.2022.09.044.
3. Moore, K.S.; Moore, R.; Fulmer, D.B.; Guo, L.; Gensemer, C.; Stairley, R.; Glover, J.; Beck, T.C.; Morningstar, J.E.; Biggs, R.; et al. DCHS1, Lix1L, and the Septin Cytoskeleton: Molecular and Developmental Etiology of Mitral Valve Prolapse. JCDD 2022, 9, 62, doi:10.3390/jcdd9020062.
4. Durst, R.; Sauls, K.; Peal, D.S.; deVlaming, A.; Toomer, K.; Leyne, M.; Salani, M.; Talkowski, M.E.; Brand, H.; Perrocheau, M.; et al. Mutations in DCHS1 Cause Mitral Valve Prolapse. Nature 2015, 525, 109–113, doi:10.1038/nature14670.
5. Sauls, K.; de Vlaming, A.; Harris, B.S.; Williams, K.; Wessels, A.; Levine, R.A.; Slaugenhaupt, S.A.; Goodwin, R.L.; Pavone, L.M.; Merot, J.; et al. Developmental Basis for Filamin-A-Associated Myxomatous Mitral Valve Disease. *Cardiovasc Res* **2012**, *96*, 109–119, doi:10.1093/cvr/cvs238.
6. Delwarde, C.; Capoulade, R.; Mérot, J.; Le Scouarnec, S.; Bouatia-Naji, N.; Yu, M.; Huttin, O.; Selton-Suty, C.; Sellal, J.-M.; Piriou, N.; et al. Genetics and Pathophysiology of Mitral Valve Prolapse. *Front. Cardiovasc. Med.* **2023**, *10*, 1077788, doi:10.3389/fcvm.2023.1077788.
7. Clemenceau, A.; Bérubé, J.; Bélanger, P.; Gaudreault, N.; Lamontagne, M.; Toubal, O.; Clavel, M.; Capoulade, R.; Mathieu, P.; Pibarot, P.; et al. Deleterious Variants in *DCHS 1* Are Prevalent in Sporadic Cases of Mitral Valve Prolapse. *Molec Gen & Gen Med* **2018**, *6*, 114–120, doi:10.1002/mgg3.347.
8. Monaghan, M.G.; Linneweh, M.; Liebscher, S.; Van Handel, B.; Layland, S.L.; Schenke-Layland, K. Endocardial-to-Mesenchymal Transformation and Mesenchymal Cell Colonization at the Onset of Human Cardiac Valve Development. *Development* **2016**, *143*, 473–482, doi:10.1242/dev.133843.
9. Camenisch, T.D.; Schroeder, J.A.; Bradley, J.; Klewer, S.E.; McDonald, J.A. Heart-Valve Mesenchyme Formation Is Dependent on Hyaluronan-Augmented Activation of ErbB2–ErbB3 Receptors. *Nat Med* **2002**, *8*, 850–855, doi:10.1038/nm742.
10. Enciso, J.M.; Gratzinger, D.; Camenisch, T.D.; Canosa, S.; Pinter, E.; Madri, J.A. Elevated Glucose Inhibits VEGF-A–Mediated Endocardial Cushion Formation. *J Cell Biol* **2003**, *160*, 605–615, doi:10.1083/jcb.200209014

11. Kim, K.; Lee, D. ERBB3-Dependent AKT and ERK Pathways Are Essential for Atrioventricular Cushion Development in Mouse Embryos. *PLoS ONE* **2021**, *16*, e0259426, doi:10.1371/journal.pone.0259426.
12. Butcher, J.T.; McQuinn, T.C.; Sedmera, D.; Turner, D.; Markwald, R.R. Transitions in Early Embryonic Atrioventricular Valvular Function Correspond With Changes in Cushion Biomechanics That Are Predictable by Tissue Composition. *Circ Res* **2007**, *100*, 1503–1511, doi:10.1161/CIRCRESAHA.107.148684.
13. Buskohl, P.R.; Gould, R.A.; Butcher, J.T. Quantification of Embryonic Atrioventricular Valve Biomechanics during Morphogenesis. *J Biomech* **2012**, *45*, 895–902, doi:10.1016/j.jbiomech.2011.11.032
14. Heckel, E.; Boselli, F.; Roth, S.; Krudewig, A.; Belting, H.-G.; Charvin, G.; Vermot, J. Oscillatory Flow Modulates Mechanosensitive Klf2a Expression through Trpv4 and Trpp2 during Heart Valve Development. *Curr Biol* **2015**, *25*, 1354–1361, doi:10.1016/j.cub.2015.03.038
15. Donat, S.; Lourenço, M.; Paolini, A.; Otten, C.; Renz, M.; Abdelilah-Seyfried, S. Heg1 and Ccm1/2 Proteins Control Endocardial Mechanosensitivity during Zebrafish Valvulogenesis. *eLife* **2018**, *7*, e28939, doi:10.7554/eLife.28939.
16. Gunawan, F.; Gentile, A.; Gauvrit, S.; Stainier, D.Y.R.; Bensimon-Brito, A. Nfatc1 Promotes Interstitial Cell Formation During Cardiac Valve Development in Zebrafish. *Circ Res* **2020**, *126*, 968–984, doi:10.1161/CIRCRESAHA.119.315992.
17. Bassen, D.; Wang, M.; Pham, D.; Sun, S.; Rao, R.; Singh, R.; Butcher, J. Hydrostatic Mechanical Stress Regulates Growth and Maturation of the Atrioventricular Valve. *Development* **2021**, *148*, dev196519, doi:10.1242/dev.196519.
18. Wang, M.; Lin, B.Y.; Sun, S.; Dai, C.; Long, F.; Butcher, J.T. Shear and Hydrostatic Stress Regulate Fetal Heart Valve Remodeling through YAP-Mediated Mechanotransduction. *eLife* **2023**, *12*, e83209, doi:10.7554/eLife.83209.
19. Gould, R.A.; Yalcin, H.C.; MacKay, J.L.; Sauls, K.; Norris, R.; Kumar, S.; Butcher, J.T. Cyclic Mechanical Loading Is Essential for Rac1-Mediated Elongation and Remodeling of the Embryonic Mitral Valve. *Curr Biol* **2016**, *26*, 27–37, doi:10.1016/j.cub.2015.11.033.
20. Vermot, J.; Forouhar, A.S.; Liebling, M.; Wu, D.; Plummer, D.; Gharib, M.; Fraser, S.E. Reversing Blood Flows Act through Klf2a to Ensure Normal Valvulogenesis in the Developing Heart. *PLoS Biol* **2009**, *7*, e1000246, doi:10.1371/journal.pbio.1000246.
21. Goddard, L.M.; Duchemin, A.-L.; Ramalingan, H.; Wu, B.; Chen, M.; Bamezai, S.; Yang, J.; Li, L.; Morley, M.P.; Wang, T.; et al. Hemodynamic Forces Sculpt Developing Heart Valves through a KLF2-WNT9B Paracrine Signaling Axis. *Dev Cell* **2017**, *43*, 274-289.e5, doi:10.1016/j.devcel.2017.09.023.
22. Vignes, H.; Vagena-Pantoula, C.; Prakash, M.; Fukui, H.; Norden, C.; Mochizuki, N.; Jug, F.; Vermot, J. Extracellular Mechanical Forces Drive Endocardial Cell Volume Decrease during Zebrafish Cardiac Valve Morphogenesis. *Dev Cell* **2022**, *57*, 598-609.e5, doi:10.1016/j.devcel.2022.02.011.
23. Oosthoek, P.W.; Wenink, A.C.G.; Vrolijk, B.C.M.; Wisse, L.J.; DeRuiter, M.C.; Poelmann, R.E.; Gittenberger-de Groot, A.C. Development of the Atrioventricular Valve Tension Apparatus in the Human Heart. *Anat Embryol* **1998**, *198*, 317–329, doi:10.1007/s004290050187.
24. Kruithof, B.P.T.; Krawitz, S.A.; Gaussin, V. Atrioventricular Valve Development during Late Embryonic and Postnatal Stages Involves Condensation and Extracellular Matrix Remodeling. *Dev Biol* **2007**, *302*, 208–217, doi:10.1016/j.ydbio.2006.09.024
25. Peacock, J.D.; Lu, Y.; Koch, M.; Kadler, K.E.; Lincoln, J. Temporal and Spatial Expression of Collagens during Murine Atrioventricular Heart Valve Development and Maintenance. *Dev. Dyn.* **2008**, *237*, 3051–3058, doi:10.1002/dvdy.21719
26. de Lange, F.J.; Moorman, A.F.M.; Anderson, R.H.; Männer, J.; Soufan, A.T.; Vries, C. de G.; Schneider, M.D.; Webb, S.; van den Hoff, M.J.B.; Christoffels, V.M. Lineage and Morphogenetic Analysis of the Cardiac Valves. *Circ Res* **2004**, *95*, 645–654, doi:10.1161/01.RES.0000141429.13560.
27. Lincoln, J.; Alfieri, C.M.; Yutzey, K.E. Development of Heart Valve Leaflets and Supporting Apparatus in Chicken and Mouse Embryos. Dev. Dyn. **2004**, 230, 239–250, doi:10.1002/dvdy.20051.
28. Norris, R.A.; Kern, C.B.; Wessels, A.; Moralez, E.I.; Markwald, R.R.; Mjaatvedt, C.H. Identification and Detection of the Periostin Gene in Cardiac Development. *Anat. Rec.* **2004**, *281A*, 1227–1233, doi:10.1002/ar.a.20135.
29. Morse, D.E.; Hamlett, W.C.; Noble, C.W. Morphogenesis of Chordae Tendineae. I: Scanning Electron Microscopy. *Anat. Rec.* **1984**, *210*, 629–638, doi:10.1002/ar.1092100410.
30. Tan, H.; Junor, L.; Price, R.L.; Norris, R.A.; Potts, J.D.; Goodwin, R.L. Expression and Deposition of Fibrous Extracellular Matrix Proteins in Cardiac Valves during Chick Development. *Microsc Microanal* **2011**, *17*, 91–100, doi:10.1017/S1431927610094365.
31. Stephens, E.H.; Grande-Allen, K.J. Age-Related Changes in Collagen Synthesis and Turnover in Porcine Heart Valves. *J Heart Valve Dis* **2007**, *16*, 11

32. Kasyanov, V.; Moreno-Rodriguez, R.A.; Kalejs, M.; Ozolanta, I.; Stradins, P.; Wen, X.; Yao, H.; Mironov, V. Age-Related Analysis of Structural, Biochemical and Mechanical Properties of the Porcine Mitral Heart Valve Leaflets. *Connec Tissue Res* **2013**, *54*, 394–402, doi:10.3109/03008207.2013.823954.
33. Stephens, E.H.; Post, A.D.; Laucirica, D.R.; Grande-Allen, K.J. Perinatal Changes in Mitral and Aortic Valve Structure and Composition. *Pediatr Dev Pathol* **2010**, *13*, 447–458, doi:10.2350/09-11-0749-OA.1.
34. Chakraborty, S.; Wirrig, E.E.; Hinton, R.B.; Merrill, W.H.; Spicer, D.B.; Yutzey, K.E. Twist1 Promotes Heart Valve Cell Proliferation and Extracellular Matrix Gene Expression during Development in Vivo and Is Expressed in Human Diseased Aortic Valves. *Dev Biol* **2010**, *347*, 167–179, doi:10.1016/j.ydbio.2010.08.021.
35. Norris, R.A.; Moreno-Rodriguez, R.A.; Sugi, Y.; Hoffman, S.; Amos, J.; Hart, M.M.; Potts, J.D.; Goodwin, R.L.; Markwald, R.R. Periostin Regulates Atrioventricular Valve Maturation. *Dev Biol* **2008**, *316*, 200–213, doi:10.1016/j.ydbio.2008.01.003.
36. Aikawa, E.; Whittaker, P.; Farber, M.; Mendelson, K.; Padera, R.F.; Aikawa, M.; Schoen, F.J. Human Semilunar Cardiac Valve Remodeling by Activated Cells From Fetus to Adult: Implications for Postnatal Adaptation, Pathology, and Tissue Engineering. *Circulation* **2006**, *113*, 1344–1352, doi:10.1161/CIRCULATIONAHA.105.591768
37. Votteler, M.; Berrio, D.A.C.; Horke, A.; Sabatier, L.; Reinhardt, D.P.; Nsair, A.; Aikawa, E.; Schenke-Layland, K. Elastogenesis at the Onset of Human Cardiac Valve Development. *Development* **2013**, *140*, 2345–2353, doi:10.1242/dev.093500.
38. Gaussin, V.; Morley, G.E.; Cox, L.; Zwijsen, A.; Vance, K.M.; Emile, L.; Tian, Y.; Liu, J.; Hong, C.; Myers, D.; et al. Alk3/Bmpr1a Receptor Is Required for Development of the Atrioventricular Canal Into Valves and Annulus Fibrosus. *Circ Res* **2005**, *97*, 219–226, doi:10.1161/01.RES.0000177862.85474.63.
39. Dickinson, M.G.; Vesely, I. Structural Changes of Rat Mitral Valve Chordae Tendineae During Postnatal Development. J Heart Valve Dis **2012**, 21, 7.
40. Aldous, I.G.; Lee, J.M.; Wells, S.M. Differential Changes in the Molecular Stability of Collagen from the Pulmonary and Aortic Valves During the Fetal-to-Neonatal Transition. *Ann Biomed Eng* **2010**, *38*, 3000–3009, doi:10.1007/s10439-010-0061-z.
41. Merryman, W.D.; Youn, I.; Lukoff, H.D.; Krueger, P.M.; Guilak, F.; Hopkins, R.A.; Sacks, M.S. Correlation between Heart Valve Interstitial Cell Stiffness and Transvalvular Pressure: Implications for Collagen Biosynthesis. *Am J Physiol-Heart C* **2006**, *290*, H224–H231, doi:10.1152/ajpheart.00521.2005
42. Hinton, R.B.; Alfieri, C.M.; Witt, S.A.; Glascock, B.J.; Khoury, P.R.; Benson, D.W.; Yutzey, K.E. Mouse Heart Valve Structure and Function: Echocardiographic and Morphometric Analyses from the Fetus through the Aged Adult. *Am J Physiol-Heart C* **2008**, *294*, H2480–H2488, doi:10.1152/ajpheart.91431.2007.
43. Filipoiu, F.M. Chapter 2: The Specific Development Period. *Atlas of Heart Anatomy and Development*; 1st ed.; Springer London: London, 2014; ISBN 978-1-4471-5381-8.
44. Aldous, I.G.; Veres, S.P.; Jahangir, A.; Lee, J.M. Differences in Collagen Cross-Linking between the Four Valves of the Bovine Heart: A Possible Role in Adaptation to Mechanical Fatigue. *Am J Physiol-Heart C* **2009**, *296*, H1898–H1906, doi:10.1152/ajpheart.01173.2008.
45. Evans, H.E.; Sack, W.O. Prenatal Development of Domestic and Laboratory Mammals: Growth Curves, External Features and Selected References. *Anatom Histol Embryol* **1973**, *2*, 11–45, doi:10.1111/j.1439-0264.1973.tb00253.x.
46. Pierlot, C.M.; Moeller, A.D.; Lee, J.M.; Wells, S.M. Biaxial Creep Resistance and Structural Remodeling of the Aortic and Mitral Valves in Pregnancy. *Ann Biomed Eng* **2015**, *43*, 1772–1785, doi:10.1007/s10439-014-1230-2
47. Pierlot, C.M.; Lee, J.M.; Amini, R.; Sacks, M.S.; Wells, S.M. Pregnancy-Induced Remodeling of Collagen Architecture and Content in the Mitral Valve. *Ann Biomed Eng* **2014**, *42*, 2058–2071, doi:10.1007/s10439-014-1077-6.
48. Pierlot, C.M.; Moeller, A.D.; Lee, J.M.; Wells, S.M. Pregnancy-Induced Remodeling of Heart Valves. *Am J Physiol-Heart C* **2015**, *309*, H1565–H1578, doi:10.1152/ajpheart.00816.2014.
49. R Core Team R: A Language and Environment for Statistical Computing 2021.
50. Fox, J.; Weisberg, S. An {R} Companion to Applied Regression 2019.
51. Jarek, S. Mvnormtest: Normality Test for Multivariate Variables 2012.
52. Signorell, A. DescTools: Tools for Descriptive Statistics. 2023.
53. Wickham, H.; Hester, J.; Chang, W.; Bryan, J. Devtools: Tools to Make Developing R Packages Easier 2022.
54. Scott, B.P. Physiological Remodelling of Mitral Valve Chordae Tendineae In The Maternal Bovine Heart, Masters, Dalhousie University: Halifax, Nova Scotia, 2016.
55. Wells, S.M.; Pierlot, C.M.; Moeller, A.D. Physiological Remodeling of the Mitral Valve during Pregnancy. Am J Physiol-Heart C **2012**, 303, H878–H892, doi:10.1152/ajpheart.00845.2011.

56. Kodigepalli, K.M.; Thatcher, K.; West, T.; Howsmon, D.P.; Schoen, F.J.; Sacks, M.S.; Breuer, C.K.; Lincoln, J. Biology and Biomechanics of the Heart Valve Extracellular Matrix. *JCDD* **2020**, *7*, 57, doi:10.3390/jcdd7040057.
57. Millington-Sanders, C.; Meir, A.; Lawrence, L.; Stolinski, C. Structure of Chordae Tendineae in the Left Ventricle of the Human Heart. *J Anatomy* **1998**, *192*, 573–581, doi:10.1046/j.1469-7580.1998.19240573.x.
58. Stephens, E.H.; de Jonge, N.; McNeill, M.P.; Durst, C.A.; Grande-Allen, K.J. Age-Related Changes in Material Behavior of Porcine Mitral and Aortic Valves and Correlation to Matrix Composition. *Tissue Eng Pt A* **2010**, *16*, 867–878, doi:10.1089/ten.tea.2009.0288.
59. Norris, R.A.; Potts, J.D.; Yost, M.J.; Junor, L.; Brooks, T.; Tan, H.; Hoffman, S.; Hart, M.M.; Kern, M.J.; Damon, B.; et al. Periostin Promotes a Fibroblastic Lineage Pathway in Atrioventricular Valve Progenitor Cells. *Dev. Dyn.* **2009**, *238*, 1052–1063, doi:10.1002/dvdy.21933
60. Chakraborty, S.; Cheek, J.; Sakthivel, B.; Aronow, B.J.; Yutzey, K.E. Shared Gene Expression Profiles in Developing Heart Valves and Osteoblast Progenitor Cells. *Physiol Genomics* **2008**, *35*, 75–85, doi:10.1152/physiolgenomics.90212.2008.
61. Fratzl, P., Chapter 2: Collagen Diversity, Synthesis and Assembly, *Collagen: Structure and Mechanics*; Ed.; Springer: New York, 2008; ISBN 978-0-387-73905-2.
62. Kalson, N.S.; Lu, Y.; Taylor, S.H.; Starborg, T.; Holmes, D.F.; Kadler, K.E. A Structure-Based Extracellular Matrix Expansion Mechanism of Fibrous Tissue Growth. *eLife* **2015**, *4*, e05958, doi:10.7554/eLife.05958.
63. Herchenhan, A.; Kalson, N.S.; Holmes, D.F.; Hill, P.; Kadler, K.E.; Margetts, L. Tenocyte Contraction Induces Crimp Formation in Tendon-like Tissue. *Biomech Model Mechanobiol* **2012**, *11*, 449–459, doi:10.1007/s10237-011-0324-0.
64. Legerlotz, K.; Dorn, J.; Richter, J.; Rausch, M.; Leupin, O. Age-Dependent Regulation of Tendon Crimp Structure, Cell Length and Gap Width with Strain. *Acta Biomater* **2014**, *10*, 4447–4455, doi:10.1016/j.actbio.2014.05.029.
65. Oryan, A.; Shoushtari, A.H. Histology and Ultrastructure of the Developing Superficial Digital Flexor Tendon in Rabbits. *Anatom Histol Embryol* **2008**, *37*, 134–140, doi:10.1111/j.1439-0264.2007.00811.x.
66. Ritz-Timme, S.; Laumeier, I.; Collins, M.J. Aspartic Acid Racemization: Evidence for Marked Longevity of Elastin in Human Skin. *Br J Dermatol* **2003**, *149*, 951–959, doi:10.1111/j.1365-2133.2003.05618.x.
67. Johnson, D.J.; Robson, P.; Hew, Y.; Keeley, F.W. Decreased Elastin Synthesis in Normal Development and in Long-Term Aortic Organ and Cell Cultures Is Related to Rapid and Selective Destabilization of mRNA for Elastin. Circ Res **1995**, *77*, 1107–1113, doi:10.1161/01.RES.77.6.1107.
68. Lincoln, J.; Alfieri, C.M.; Yutzey, K.E. BMP and FGF Regulatory Pathways Control Cell Lineage Diversification of Heart Valve Precursor Cells. *Dev Biol* **2006**, *292*, 290–302, doi:10.1016/j.ydbio.2005.12.042
69. Hinton, R.B.; Lincoln, J.; Deutsch, G.H.; Osinska, H.; Manning, P.B.; Benson, D.W.; Yutzey, K.E. Extracellular Matrix Remodeling and Organization in Developing and Diseased Aortic Valves. *Circ Res* **2006**, *98*, 1431–1438, doi:10.1161/01.RES.0000224114.65109.4e
70. Brettell, L.M.; McGowan, S.E. Basic Fibroblast Growth Factor Decreases Elastin Production by Neonatal Rat Lung Fibroblasts. *Am J Respir Cell Mol Biol* **1994**, *10*, 306–315, doi:10.1165/ajrcmb.10.3.8117449.
71. Rich, C.B.; Fontanilla, M.R.; Nugent, M.; Foster, J.A. Basic Fibroblast Growth Factor Decreases Elastin Gene Transcription through an AP1/cAMP-Response Element Hybrid Site in the Distal Promoter. J Biol Chem **1999**, 274, 33433–33439, doi:10.1074/jbc.274.47.33433.
72. Fowden, A.L.; Li, J.; Forhead, A.J. Glucocorticoids and the Preparation for Life after Birth: Are There Long-Term Consequences of the Life Insurance? *Proc. Nutr. Soc.* **1998**, *57*, 113–122, doi:10.1079/PNS19980017.
73. Rich, C.B.; Goud, H.D.; Bashir, M.; Rosenbloom, J.; Foster, J.A. Developmental Regulation of Aortic Elastin Gene Expression Involves Disruption of an IGF-I Sensitive Repressor Complex. Biochem Bioph Res Co **1993**, 196, 1316–1322, doi:10.1006/bbrc.1993.2396.
74. Pierce, R.A.; Mariencheck, W.I.; Sandefur, S.; Crouch, E.C.; Parks, W.C. Glucocorticoids Upregulate Tropoelastin Expression during Late Stages of Fetal Lung Development. Am J Physiol-Lung C **1995**, 268, L491–L500, doi:10.1152/ajplung.1995.268.3.L491.